

ED6001 Project Report

Optic Disc and Cup Segmentation Methods

25.11.2020

By Chella Thiyagarajan N ME17B179

Objective

The objective of this project is to review Optic disc and cup segmentation papers on a medical image dataset using popular deep learning architectures and various image processing methods. The dataset is provided by the Aravind Eye Hospital, Madurai.

Introduction

Glaucoma is the second leading cause of loss of vision in the world. Examining the head of the optic nerve (cup-to-disc ratio) is very important for diagnosing glaucoma and for patient monitoring after diagnosis. Images of the optic disc and optic cup are acquired by fundus camera as well as Optical Coherence Tomography. The optic disc and optic cup segmentation techniques are used to isolate the relevant parts of the retinal image and to calculate the cup-to-disc ratio. The main objective of this paper is to review segmentation methodologies and techniques for the disc and cup boundaries which are utilized to calculate the disc and cup geometrical parameters automatically and accurately to help the professionals in glaucoma to have a wide view and more details about the optic nerve head structure using retinal fundus images. We provide a brief description of each technique, highlighting its performance metrics.

A retinal fundus image is an image which contains the interior surface of the eye, which includes retina, optic nerve head, macula, fovea and blood vessels. The interior surface of the eye has a bright circular region called as optic nerve head (ONH). The blood vessels and optic nerve fibers exit the retina through ONH. The ONH further contains optic disc and optic cup. The optic cup is the brightest region inside ONH. In a normal eye, the ONH has only optic disc. However, for a glaucoma affected eye, the cupping of disc starts and optic cup is formed. The fundus image labeled with different parts is shown below in Figure 1.

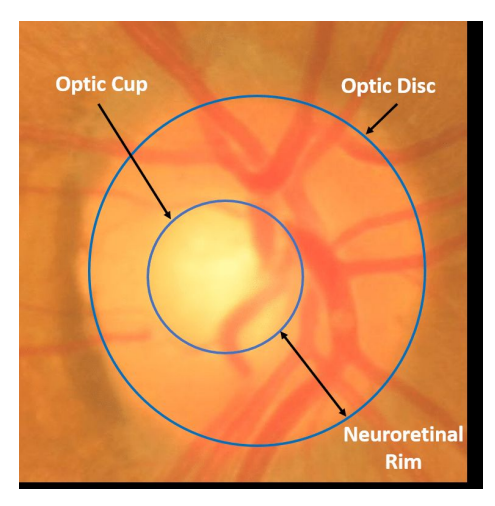


Figure 1

Description of Data

DRISHTI (Main):

Drishti-GS1 dataset consists of a total of 101 images. These have been divided into 50 training and 51 testing images. All the images have been marked by 4 eye experts with varying clinical experience. All images were collected at Aravind eye hospital, Madurai from visitors to the hospital, with their consent. Glaucoma patient selection was done by clinical investigators based on clinical findings during the visit. Selected patients were between 40-80 years of age with roughly equal number of males and females. The data collection protocol was as follows.

- All images were taken centered on OD with a Field-Of-View(FOV) of 30-degrees and of dimensions 2896 X 1944 pixels and PNG uncomressed image format.
- Groundtruth was collected from data experts with varying clinical experience of 3,5,9 and 20 years respectively.
- For the groundtruth collection a dedicated marking tool was created to allow for precise boundary marking.

RIM ONE (Supplementary):

RIM ONE-v3, from the MIAG group of the University of La Laguna (Spain), consists of 159 fundus images which have been labeled by expert ophthalmologists for both disc and cup.

Methodology from paper [1]

A colour fundus image comprises of red, green and blue channels. The optic disc is mostly of red, orange or yellow colour and because of this property it can be easily distinguished in the red channel. After studying a large number of images, it was observed that the green channel has a high contrast and this property of green channel is used to distinguish the optic cup from the optic disc.

(a). Preprocessing

The images are made ready for applying threshold by removing the information from the both the channels. The information can be removed by simply subtracting the mean and standard deviation from the channels.

The image obtained after removing information from the channels contains only the optic nerve head region in both the channels.

Preprocessed images are shown below:

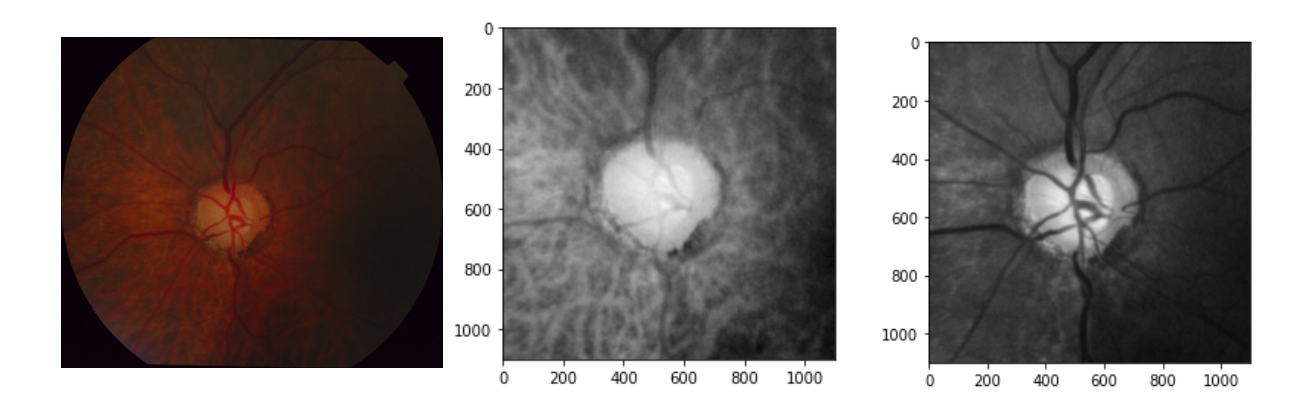


Figure 2
Image on left side is our original fundus image, Image in the middle is Red channel of the fundus image, image on right side is our Green channel of the fundus image

(b). Adaptive Threshold Based Algorithm

Figure 3 Given below is the flow chart of the methodology of how the algorithm works

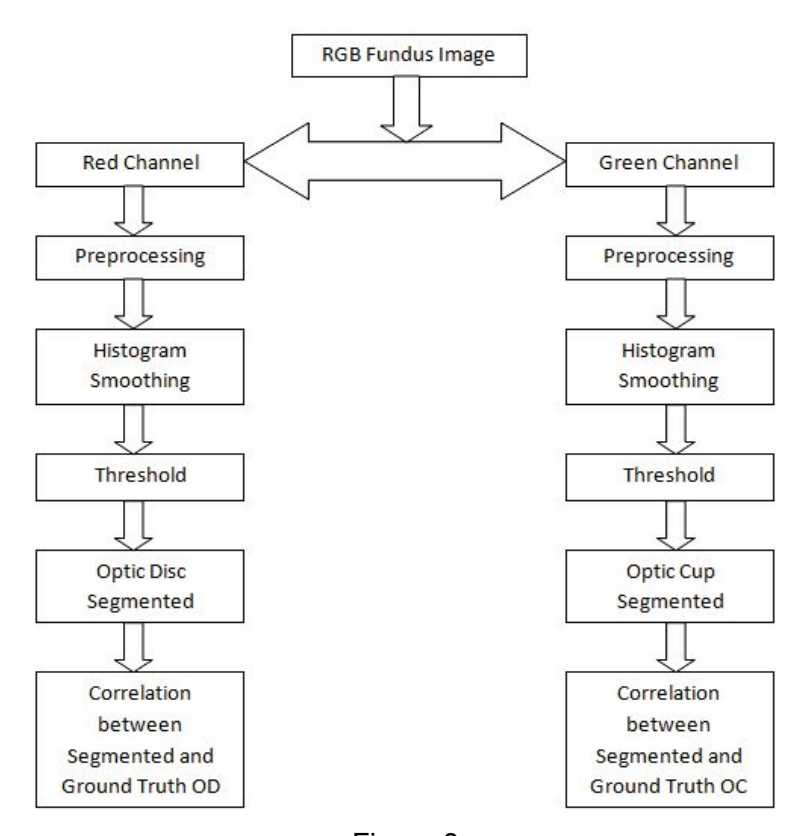


Figure 3

Histogram Smoothing:

The histogram of the preprocessed red channel is plotted and smoothed using a Gaussian window of size m×m and The histogram of the preprocessed green channel is plotted and smoothed using the same Gaussian window of size m×m.

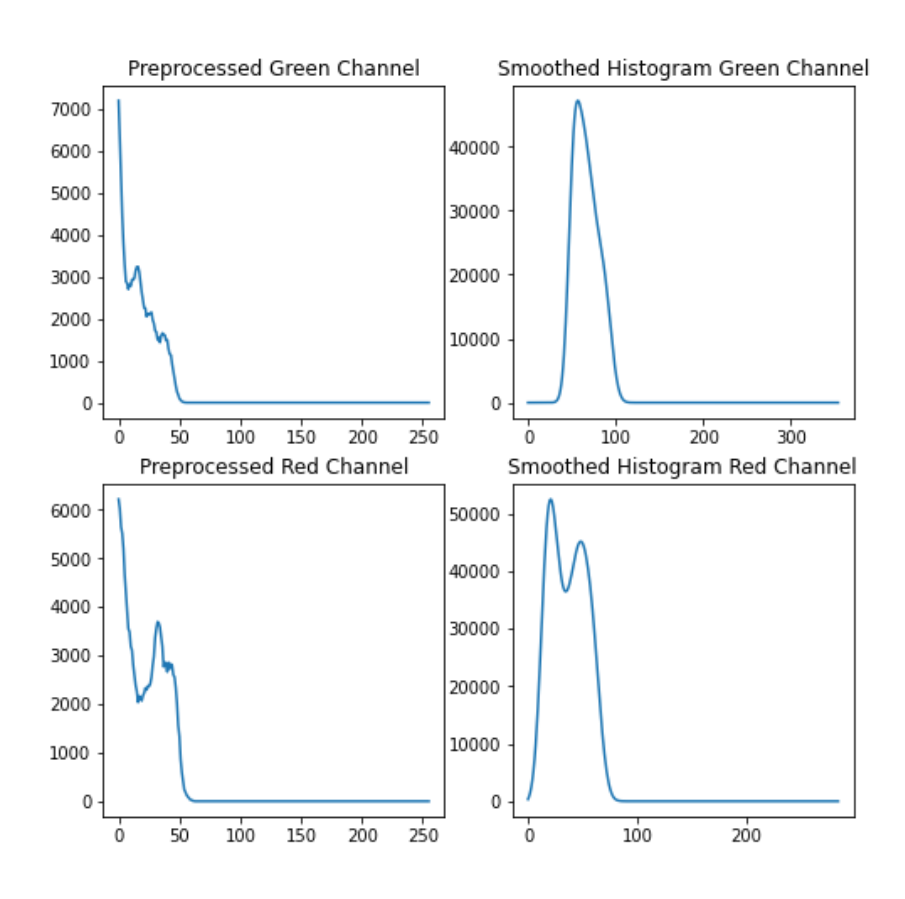


Figure 4
Color channels and it's corresponding gaussian smoothed histograms are shown

Threshold:

The adaptive threshold value is formulated from the smoothed histograms (Figure 4) and the proposed threshold values are

$$T1 = (0.5*m) - (2*\sigma_G) - (\sigma_{R1})$$

Where, T1 = threshold for segmentation of optic disc

m = size of Gaussian window

 σ_G = standard deviation of Gaussian window

 σ_{RI} = standard deviation of the preprocessed red channel

$$T2 = (0.5*m) + (2*\sigma_G) + (2*\sigma_{GI}) + (\mu_{GI})$$

Where, T2 = threshold for segmentation of optic cup

m = size of Gaussian window

 σ_G = standard deviation of Gaussian window

 σ_{GI} = standard deviation of the preprocessed green channel

 μ_{GI} = mean of the preprocessed green channel

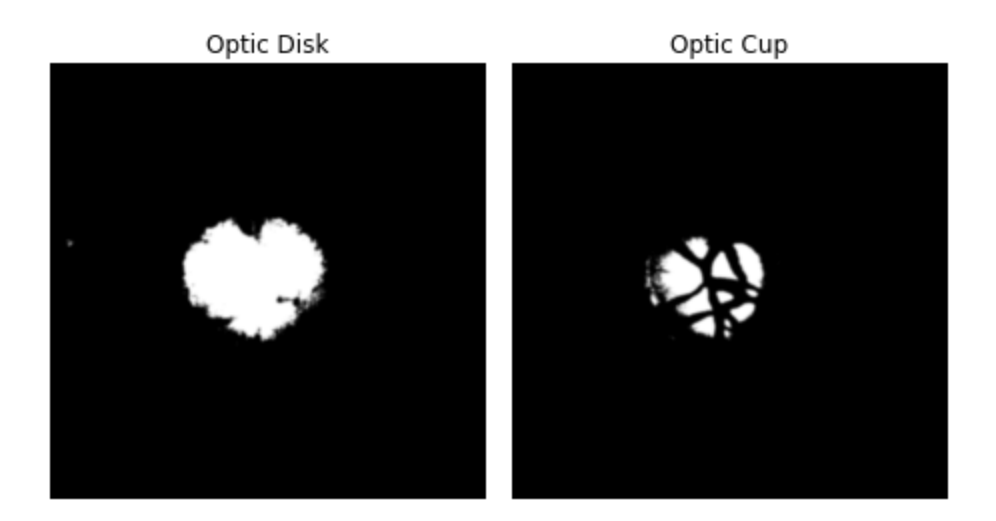


Figure 5
Out-put images after performing adaptive thresholding. Image to the left correspond to optic disc and to the right correspond to optic cup

Optic Disc and Cup Segmentation:

The Thresholded optic disc and cup are subjected to morphology operations. Firstly, a morphological closing is performed followed by a morphological opening. An ellipse-shaped structuring element is used to perform the morphological operations. We later find an ellipse contour that fits around the segmented cup and disk for easier radius calculations.

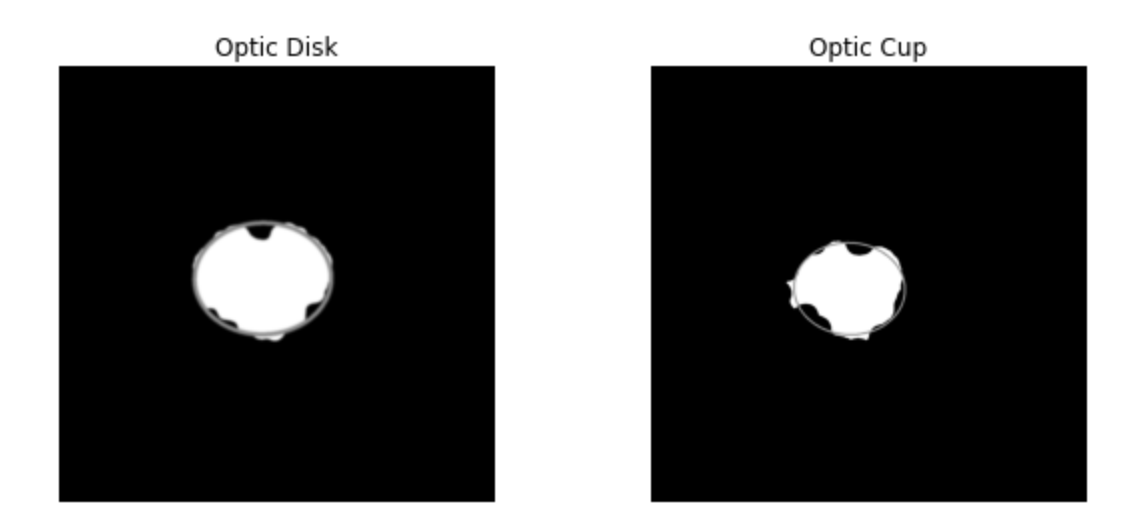


Figure 6
Out-put images after performing various morphing operations and fitting ellipse using contour functions. Image to the left correspond to optic disc and to the right correspond to optic cup.

CDR Calculations:

The major axis of the obtained contours are considered as the diameters of the cup and disk and with these values, we can calculate the CDR value. The formula for CDR metric is given as

CDR = radius of cup / radius of disk

Sample Results of 5 images are shown in Figure 7

40	File Code	Expert1	Expert2	Expert3	Expert4	predicted cdr
0	_001	0.85	0.82	0.80	0.82	0.674107
1	_001	0.85	0.82	0.80	0.82	0.674107
2	_003	0.83	0.79	0.72	0.79	0.832386
3	_005	0.86	0.87	0.81	0.80	0.757225
4	_006	0.64	0.77	0.65	0.53	0.342391

Figure 7

Conclusion:

The proposed methodology to segment the optic disc and cup from a fundus image is barely accurate and very efficient. The common challenge in glaucoma detection is the accurate segmentation of optic discs which can be affected due to presence of peripapillary atrophy (PPA). However, in the proposed work, this shortcoming is overcome as only the brighter pixels will be threshold.

However, The algorithm failed on 9-12 images in our DRISHTI dataset due to inappropriate framing and brighter pixels that affect cup segmentations. The above approach cannot be automated smoothly as many hyper parameters and human interventions are required. The CDR accuracy which we obtained from the DRISHTI dataset is 86.3% which is pretty low than the claimed value. Boundaries that we obtained from discs and cups are susceptible to errors which are induced by morphological operations. Morphological operations tries to fill the areas in the cup which are left dark but this computational morphing distorts the shape and further affects CDR calculations.

Methodology from paper [2]

Given below is the flowchart of the methodology of how the paper is implemented

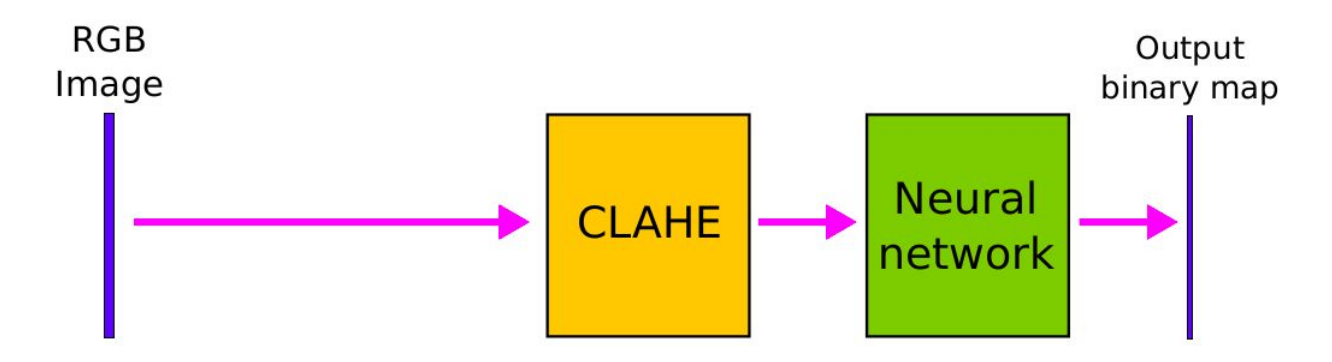


Figure 8
Pipe-line for segmentation of Optic Disc

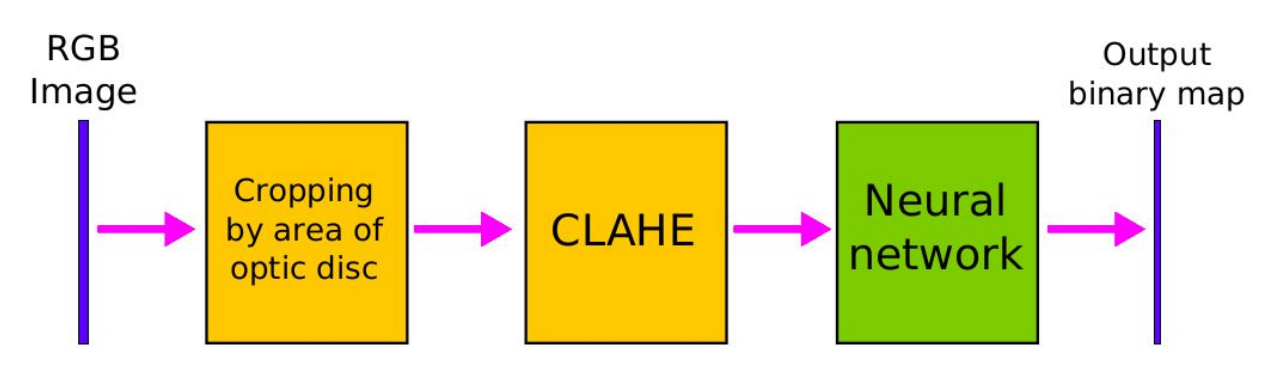


Figure 9
Pipe-line for segmentation of Optic Cup

Data Selection:

We all know that to improve the performance of the Artificial Neural Network we need more data. DRISHTI-GS only has 51 images on the training set which is very low in number, Therefore we try to use it along with RIM-ONE dataset solely for the purpose of increasing the size of the training set.

RIM-ONE: RIM-ONE allows the free download of different fundus images (healthy eyes and eyes with different glaucoma levels), contains gold standards for each image and proposes a common methodology for comparing segmentation results with the gold standard. This reference image database for glaucoma is part of a research project developed in collaboration with three Spanish hospitals: Hospital Universitario de Canarias, Hospital Clínico San Carlos

and Hospital Universitario Miguel Servet. The aim of the project is the design of an automated software system for supporting glaucoma diagnosis.

We use publicly available RIM-ONE v3, DRISHTI datasets. The use of multiple datasets both for training and for validation allows our system to be more independent of the capture devices than other available implementations.

Data Preprocessing:

Contrast Limited Adaptive Histogram Equalization (CLAHE) is used as a pre-processing step for both cup and disk. It equalizes contrast by changing color of image regions and interpolating the result across them. For optic cup, we firstly crop the images by bounding box of optic disc (with margin from each side), which can be acquired from trained algorithm for optic disc. The images are resized with various resolutions and saved as a hdf5 files. The Preprocessed data files are Open-sourced by [3].

Standardization:

Standardization is the process of developing, promoting and possibly mandating standards-based and compatible technologies and processes within a given industry. It refers to shifting the distribution of each attribute to have a mean of zero and a standard deviation of one (unit variance). It is useful to standardize attributes for a model that relies on the distribution of attributes such as Gaussian processes. It solves the problem of Intensity Standardization.

CLAHE:

This algorithm can be applied to improve the contrast of images and enhancing the definitions of edges in each region of an images. This algorithm works by creating several histograms of the original image, and uses all of these histograms to redistribute the lightness of the image. Adaptive histogram equalization (AHE) improves on this by transforming each pixel with a transformation function derived from a neighbourhood region. In its simplest form, each pixel is transformed based on the histogram of a square surrounding the pixel.

Image Resize:

An HDF5 dataset created with the default settings will be contiguous; in other words, laid out on disk in traditional C order. Datasets may also be created using HDF5's chunked storage layout. This means the dataset is divided up into regularly-sized pieces which are stored haphazardly on disk, and indexed using a B-tree. Chunked storage makes it possible to resize datasets, and because the data is stored fixed-size chunks, to use compression filters like 'gzip'. In HDF5, datasets can be resized once created up to a maximum size. In our case, our dataset is stored with 3 shapes such as 512x512, 256x256, and 128x128. We would use images with size 128x128 as it would have reduced computational complexity.

Cropping Operation:

For Cup segmentation, the area of interest is the region that encloses optic disc, Therefore we try to impose the optic disc ground truth on our image and try to cut a bounding box that encloses the ground truth. We get a bounding box using skimage.measure.regionprops method which measure properties of labeled image regions. Bbox is one of it's attributes which provides us a box, we further increase the box size with a gap of 20 on all the sides.

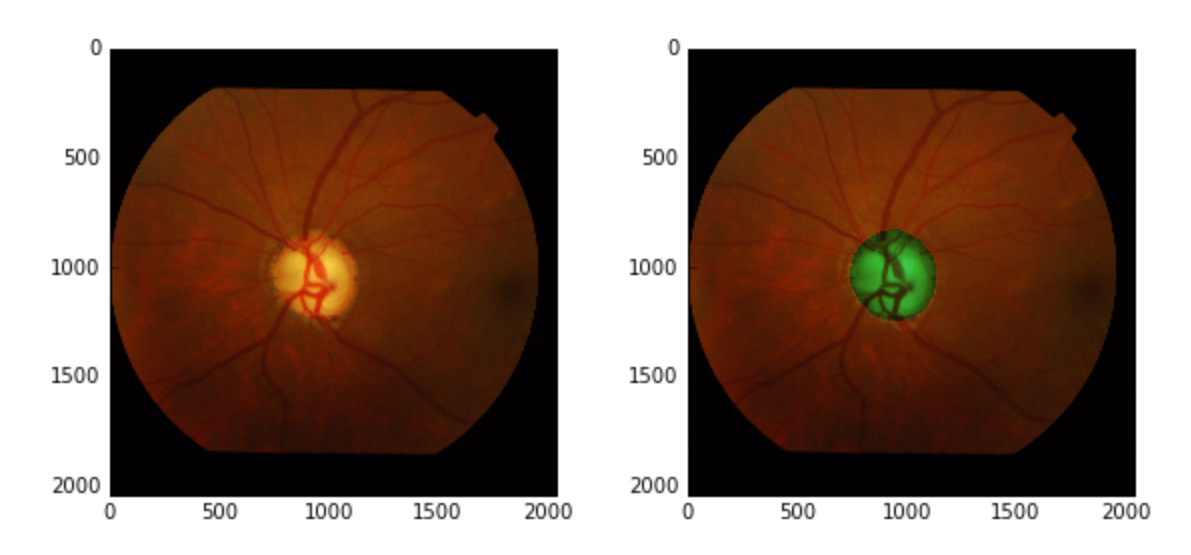


Figure 10

Left Image: Fundus image of our dataset, Right Image: Fundus image mapped with it's disc segmentation ground truth.

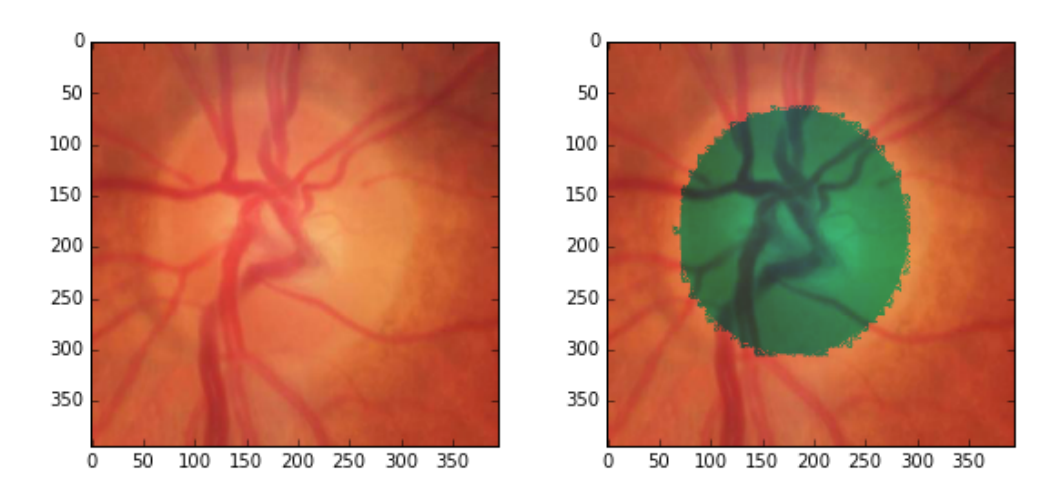


Figure 11

Left Image: Fundus image of our dataset, Right Image: Fundus image mapped with it's cup segmentation ground truth.

Training:

Model Architecture:

The U-Net architecture consists of a contracting path to capture context and a symmetric expanding path that enables precise localization. The U-Net architecture can be trained end-to-end from very few images and outperforms most of the methods on the ISBI challenge for segmentation of neuronal structures in electron microscopic stacks. The U-net architecture implemented by is shown below.

The architecture presented in the paper is depicted in Fig. 12. Like the original U-Net, it consists of contracting path (left side) and an expansive path (right side). Contracting path structurally repeats a typical architecture of convolutional part of the classification network, e.g. VGG-16. On the expansive path, information is merged from layers of contracting path of appropriate resolution and layers of expansive path of lower resolution, so that a whole network recognizes patterns at several scales. Input image is firstly passed through a convolutional layer with filters of 3 x 3 pixels spatial resolution; number of filters in a layer is shown in the figure above a blue rectangle representing layer's output. Afterwards, Dropout regularization and ReLu activation function (f(x) = max(0, x)) are applied. The same is repeated again, and Max Pooling operation is applied, reducing image width and height by two. Image is then passed through aforementioned sequence of layers multiple times, until resolution is low enough. On the expansive path, the same convolutional layers are applied, interleaved with Upsampling layers, which raise image width and height by two in a trivial way.

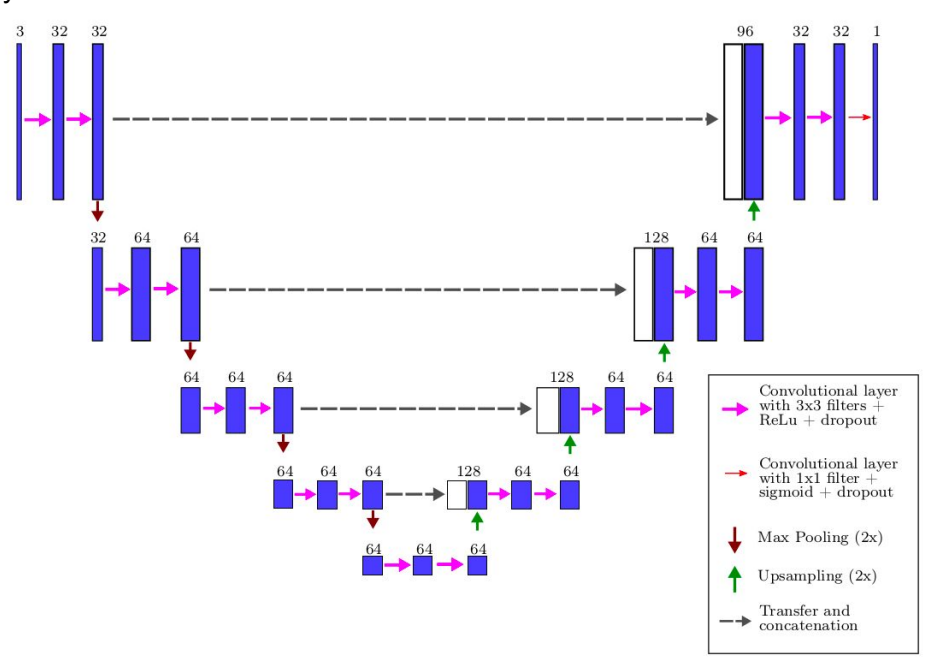


Figure 12

We use **Adam** as our optimizer function, Adam is different to classical stochastic gradient descent. Stochastic gradient descent maintains a single learning rate (termed alpha) for all weight updates and the learning rate does not change during training. Adam is a replacement optimization algorithm for stochastic gradient descent for training deep learning models. Adam is relatively easy to configure where the default configuration parameters do well on most problems.

We use **Dice Coefficient score** as our model performance evaluation metric. We validate the algorithm by calculating the Dice score, which is a measure of how similar the objects are. So it is the size of the overlap of the two segmentations divided by the total size of the two objects. Dice Score is given as d(A, B) in Figure 13. The Dice score is not only a measure of how many positives you find, but it also penalizes for the false positives that the method finds, similar to precision. so it is more similar to precision than accuracy. The only difference is the denominator, where you have the total number of positives instead of only the positives that the method finds. So the Dice score is also penalizing for the positives that your algorithm could not find.

As a loss function we use **Log Dice Loss**, which is given as I(A, B):

$$l(A, B) = -\log d(A, B), \text{ where:}$$

$$d(A, B) = \frac{2\sum_{i,j} a_{ij} b_{ij}}{\sum_{i,j} a_{ij}^2 + \sum_{i,j} b_{ij}^2},$$

where $A = (a_{ij})_{i=1}^H {}_{j=1}^W$ is a predicted output map, containing probabilities that each pixel belongs to the foreground, and $B = (b_{ij})_{i=1}^H {}_{j=1}^W$ is a correct binary output map.

Figure 13

In simple words A is the predicted segmented image and B is true segmented image.

Training and Test Set:

Both Drishti and RIM-ONE images are concatenated to form a single dataset. The concatenated dataset is then augmented using CLAHE filter and changing filters and changing various hyper parameters. Recent advances in deep learning models have been largely attributed to the quantity and diversity of data gathered in recent years. Data augmentation is a strategy that enables practitioners to significantly increase the diversity of data available for training models, without actually collecting new data. This kind of augmentation is solely to increase the size of the dataset 20 times. This data is then divided into train set and test set with test set having a 25% of the whole dataset. Later the dataset is shuffled by using random.permutation, because shuffling data serves the purpose of reducing variance and making sure that models remain general and overfit less.

Results:

Training Set Log-Dice-Loss and Test Set Log-Dice-Loss during Cup and Disc Segmentation Training:

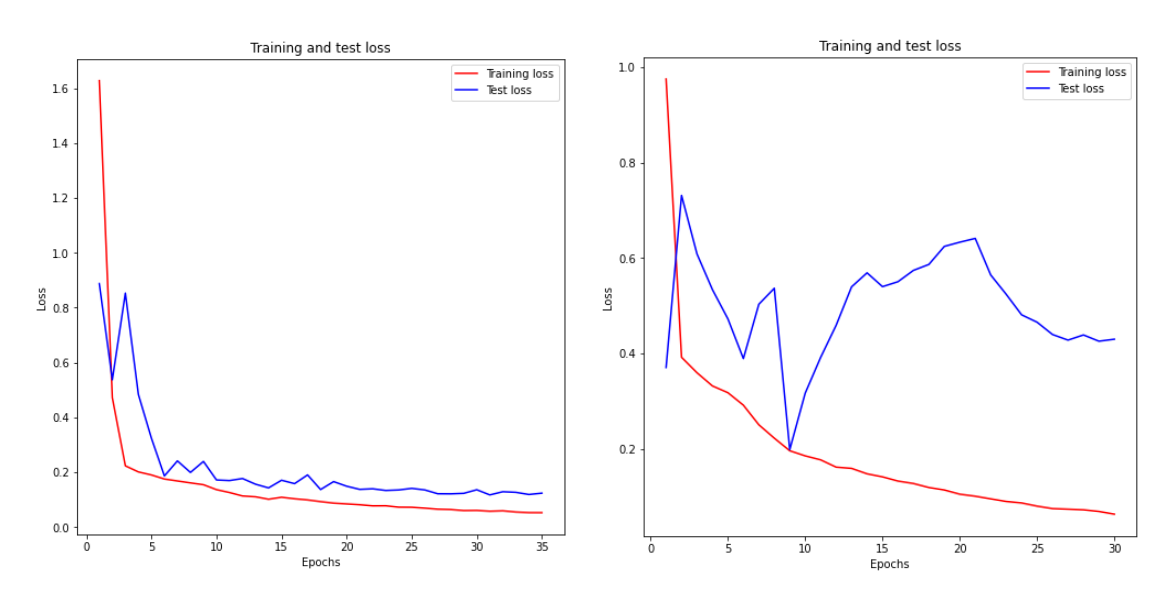


Figure 14

Left image: correspond to Disc Segmentation, Right image: correspond to cup segmentation

Training Set Dice-Score and Test Set Dice-Score during Cup and Disc Segmentation Training:

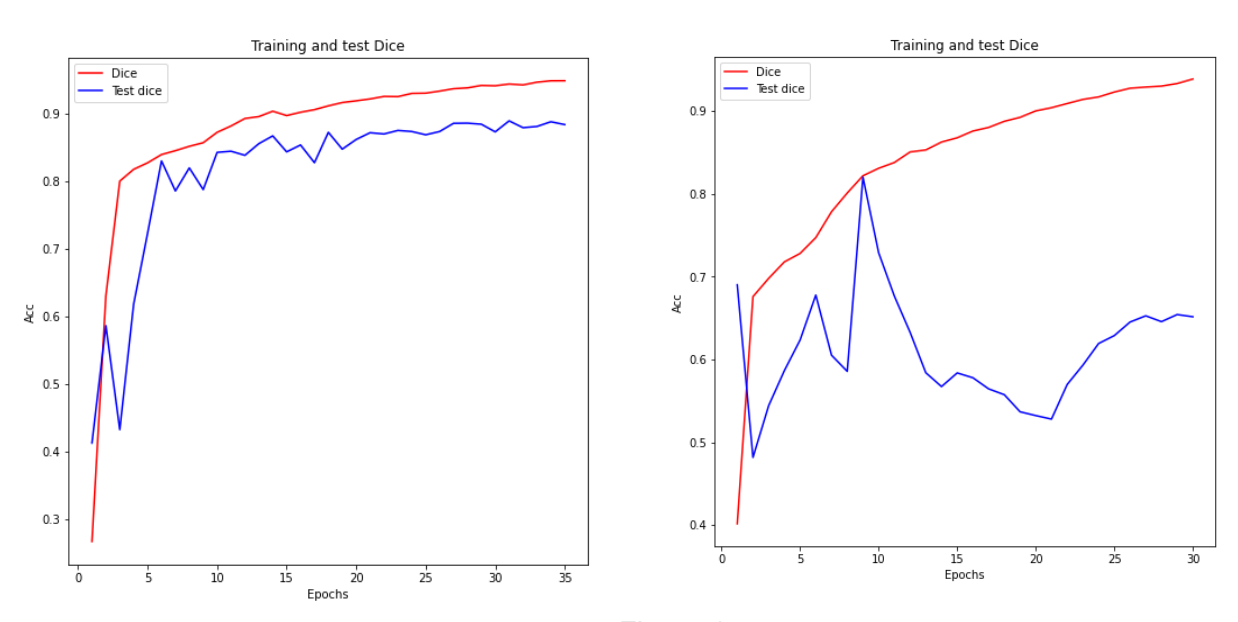


Figure 15

Left image: correspond to Disc Segmentation, Right image: correspond to cup segmentation

Disc Segmentation:

Dice and IOU Scores are calculated using RIM-ONE as our validation set:

Dice Metric:

Mean: 0.8709752

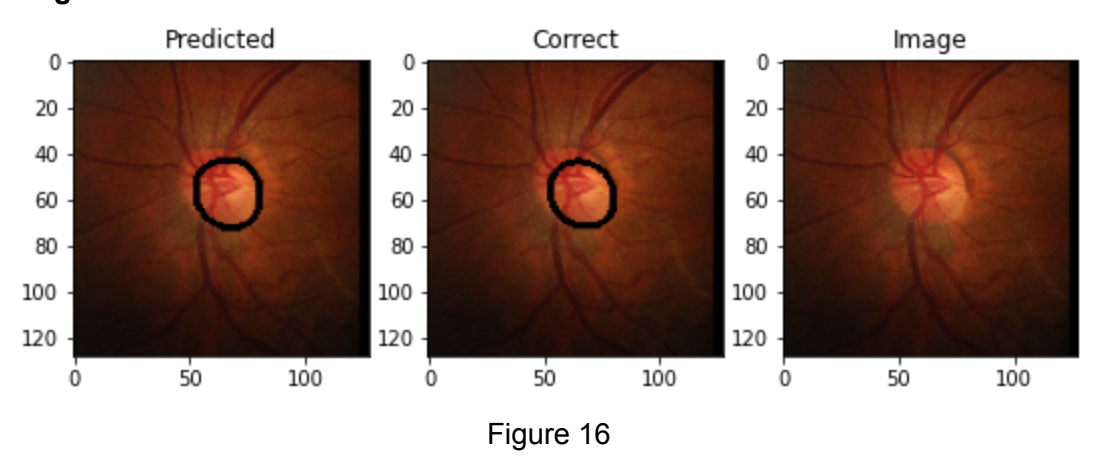
Standard Deviation: 0.06440953

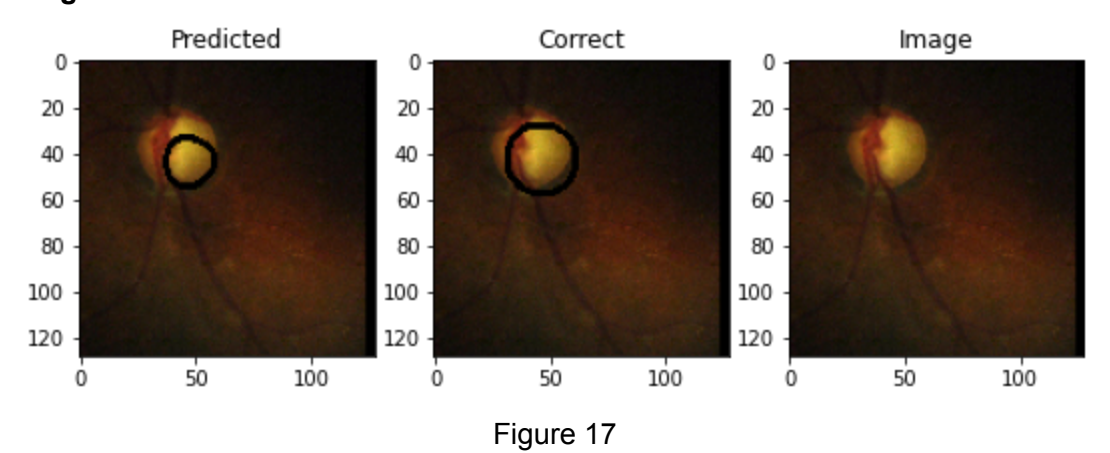
IOU Metric:

Mean: 0.7769381

Standard Deviation: 0.096645266

Model Segmentation with best Dice Score:





Disc Segmentation:

Dice and IOU Scores are calculated using DRISHTI as our validation set:

Dice Metric:

Mean: 0.91630703

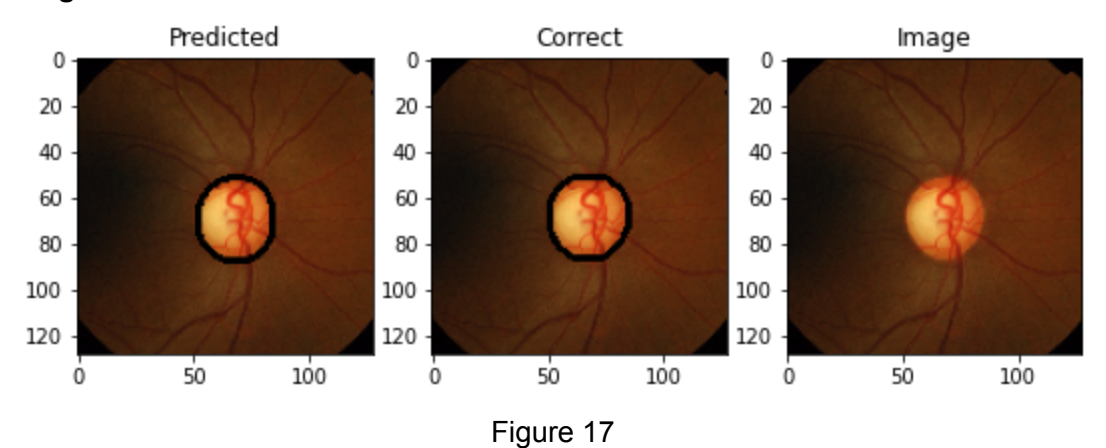
Standard Deviation: 0.025937106

IOU Metric:

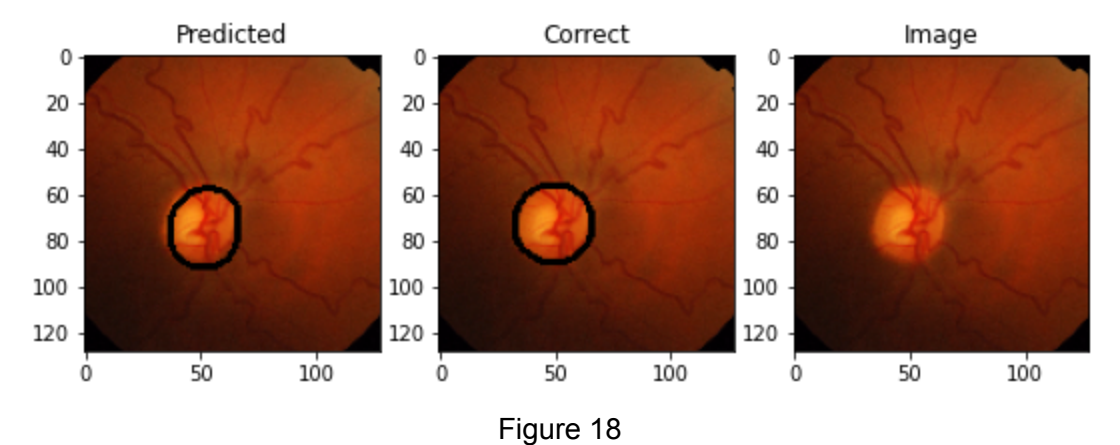
Mean: 0.84659714

Standard Deviation: 0.0441317

Model Segmentation with best Dice Score:



•



Cup Segmentation:

Dice and IOU Scores are calculated using RIM-ONE as our validation set:

Dice Metric:

Mean: 0.80241454

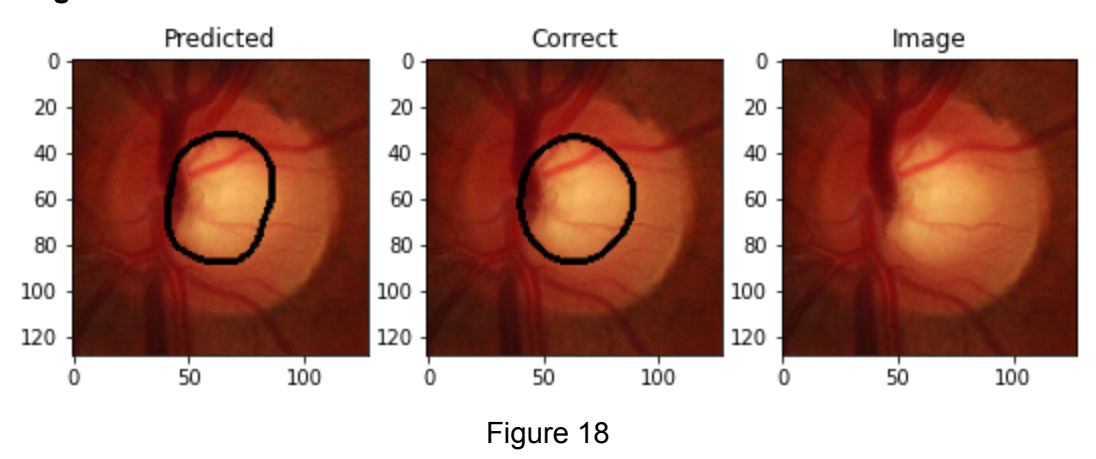
Standard Deviation: 0.09940979

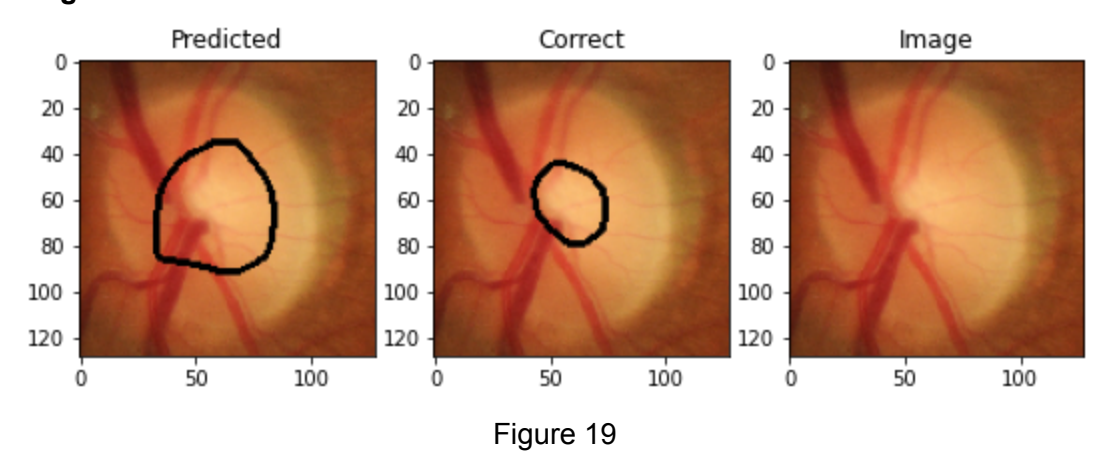
IOU Metric:

Mean: 0.6809287

Standard Deviation: 0.13192643

Model Segmentation with best Dice Score:





Cup Segmentation:

Dice and IOU Scores are calculated using DRISHTI as our validation set:

Dice Metric:

Mean: 0.90240574

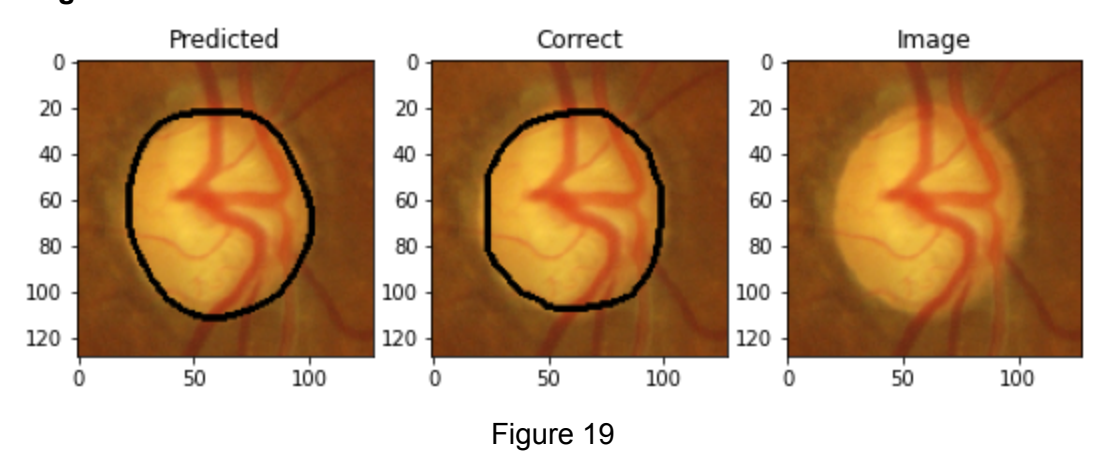
Standard Deviation: 0.07061479

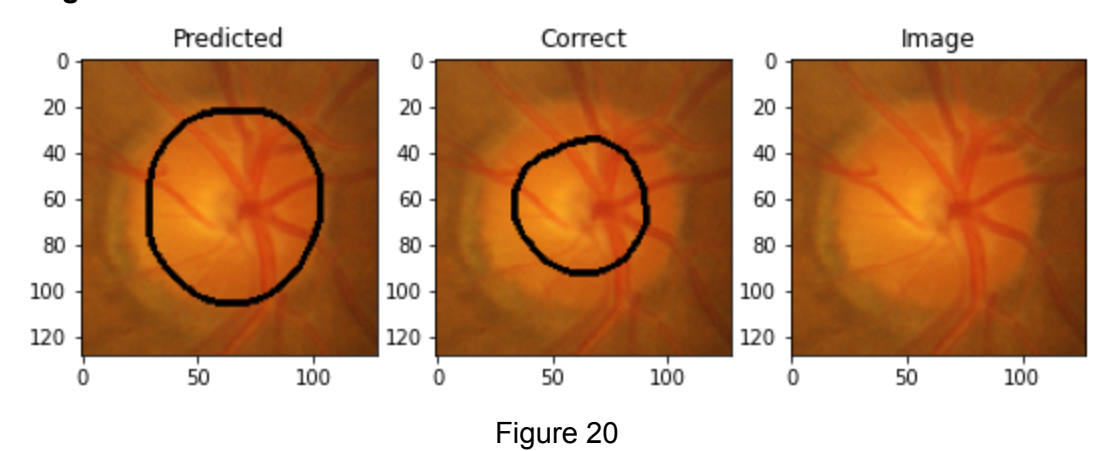
IOU Metric:

Mean: 0.8287271

Standard Deviation: 0.10222741

Model Segmentation with best Dice Score:





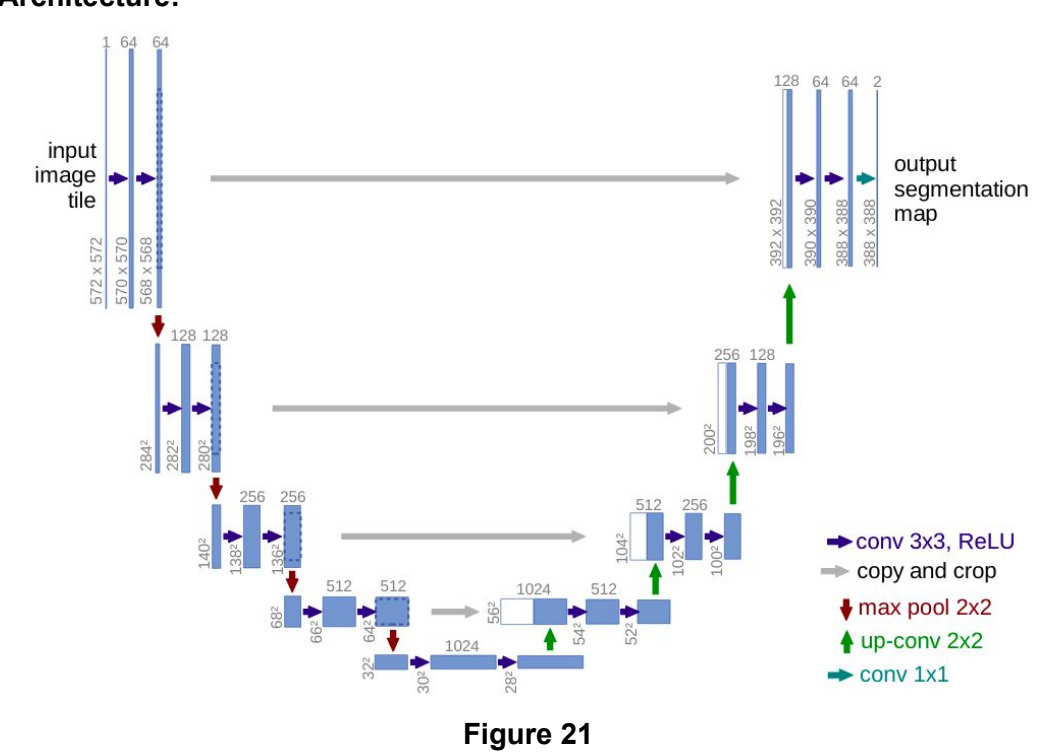
Conclusion:

U-Net neural networks can provide results similar or better than existing methods for the tasks of optic disc and cup segmentation on eye fundus images. However, we can see that the model's disc segmentation metrics are better than it's cup segmentation metrics. We also can see that after epoch 12 the model's cup segmentation accuracy drops significantly and later improves at a very slower rate, Training with high epochs may improve its accuracy optic cup is more challenging to recognize, which is supported by the fact that its border is much more subtle. There is a room for improvement for optic cup segmentation, and further research is needed

Methodology from paper [3]:

The data preprocessing and Training approaches are followed as same as Methodology of paper [2] except the model architecture. The main purpose of choosing this paper is to apply a commonly used U-net architecture to our dataset and compare the performance with our last model. Here too we use the same optimisation, loss and performance evaluation metric functions.

Model Architecture:



U-net architecture (example for 32x32 pixels in the lowest resolution). Each bluebox corresponds to a multi-channel feature map. The number of channels is denoted on top of the box. The x-y-size is provided at the lower left edge of the box. Whiteboxes represent copied feature maps. The arrows denote the different operations.

Network consists of a contracting path (left side) and an expansive path (right side). The contracting path follows the typical architecture of a convolutional network. It consists of the repeated application of two 3x3 convolutions (unpadded convolutions), each followed by a rectified linear unit (ReLU) and a 2x2 max pooling operation with stride 2 for downsampling. At each downsampling step we double the number of featured channels. Every step in the expansive path consists of an upsampling of the feature map followed by a 2x2 convolution ("up-convolution") that halves the number of feature channels, a concatenation with the correspondingly cropped feature map from the contracting path, and two 3x3 convolutions, each fol-lowed by a ReLU. The cropping is necessary due to the loss of border pixels in every convolution. At the final layer a 1x1 convolution is used to map each 64-component feature vector to the desired number of classes. In total the network has 23 convolutional layers. The input and output layer channels are modified according to our dataset.

Results: Training Set Log-Dice-Loss and Test Set Log-Dice-Loss during Cup and Disc Segmentation Training:

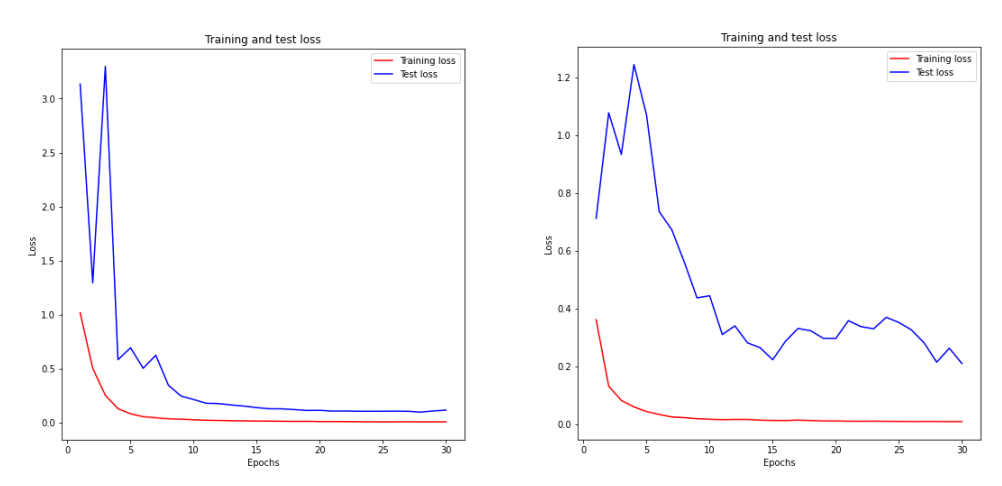
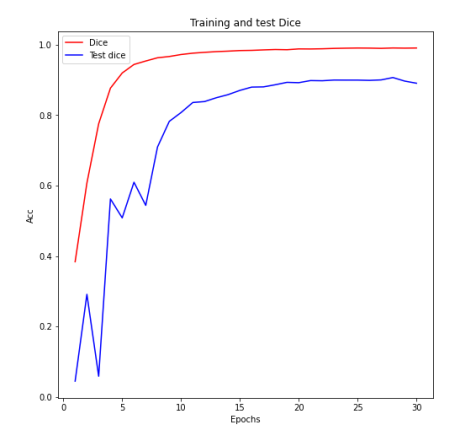
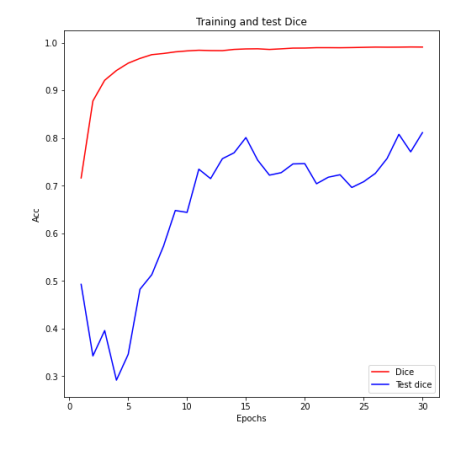


Figure 22

Left image: correspond to Disc Segmentation, Right image: correspond to cup segmentation Training Set Dice-Score and Test Set Dice-Score during Cup and Disc Segmentation Training:





Disc Segmentation:

Dice and IOU Scores are calculated using RIM-ONE as our validation set:

Dice Metric:

Mean: 0.8891012

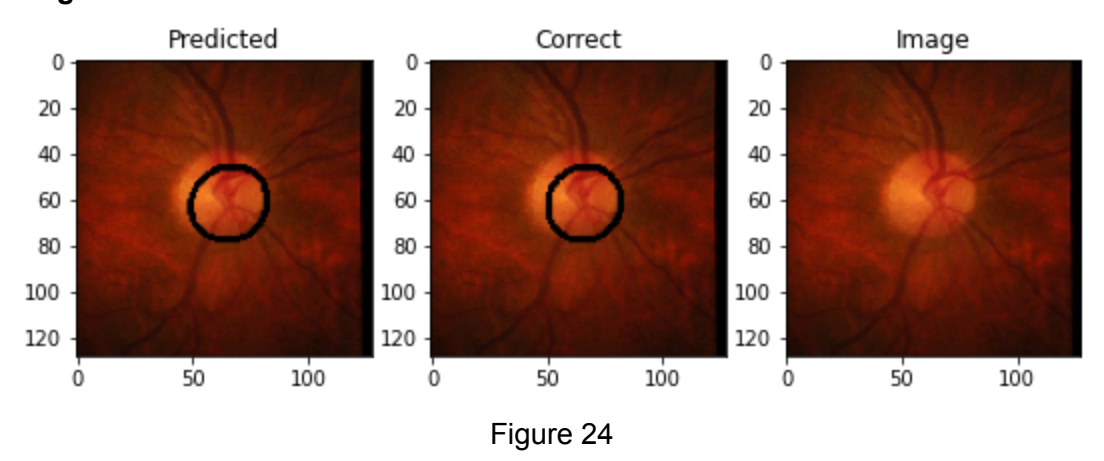
Standard Deviation: 0.18006852

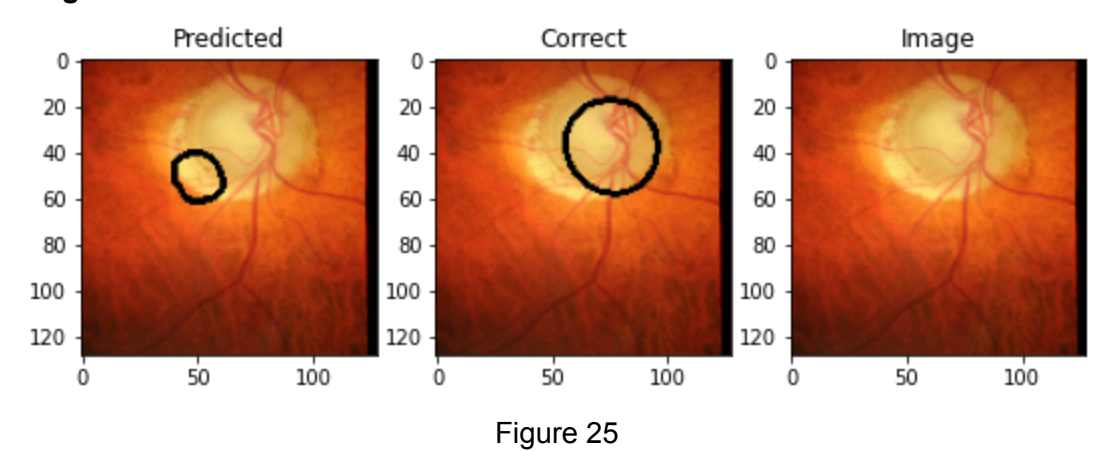
IOU Metric:

Mean: 0.829739

Standard Deviation: 0.18314674

Model Segmentation with best Dice Score:





Disc Segmentation:

Dice and IOU Scores are calculated using DRISHTI as our validation set:

Dice Metric:

Mean: 0.8997263

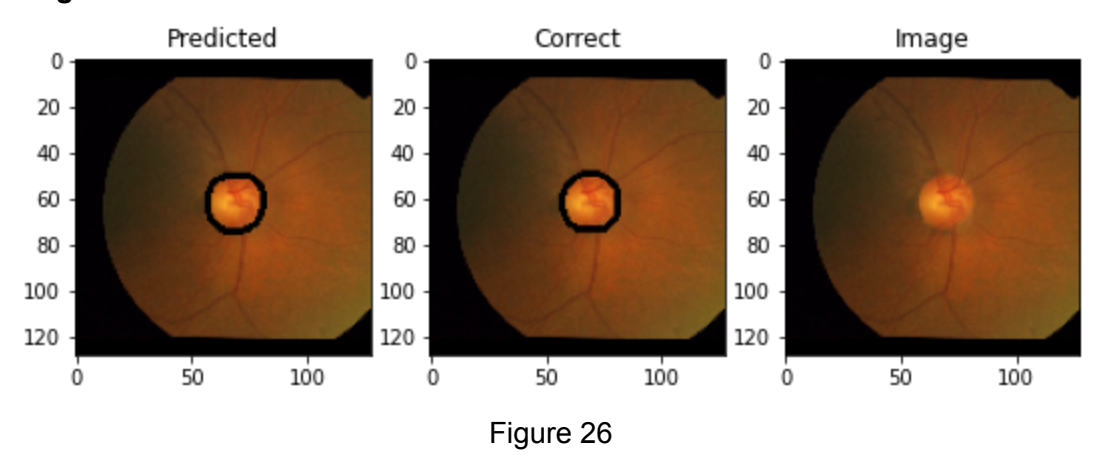
Standard Deviation: 0.054576475

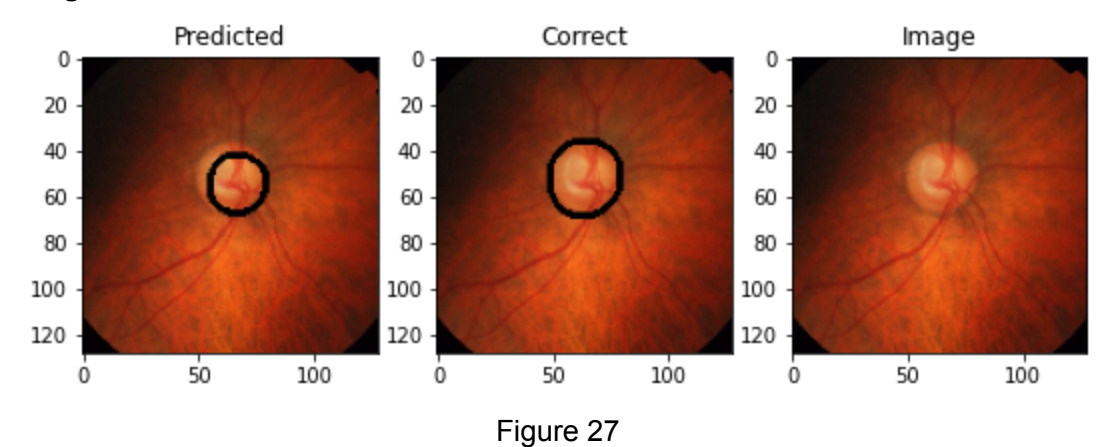
IOU Metric:

Mean: 0.8219516

Standard Deviation: 0.08528548

Model Segmentation with best Dice Score:





Cup Segmentation:

Dice and IOU Scores are calculated using RIM-ONE as our validation set:

Dice Metric:

Mean: 0.8241146

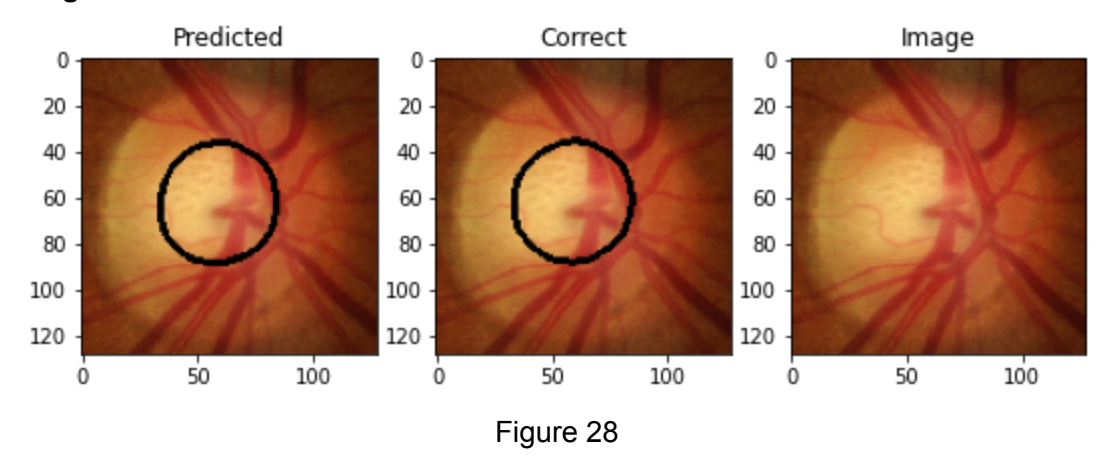
Standard Deviation: 0.100919105

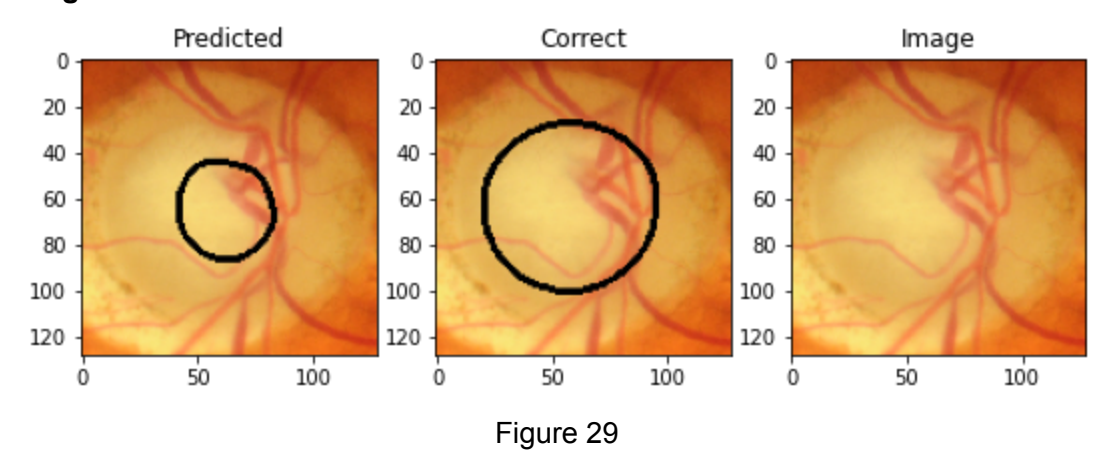
IOU Metric:

Mean: 0.71260643

Standard Deviation: 0.13796121

Model Segmentation with best Dice Score:





Cup Segmentation:

Dice and IOU Scores are calculated using DRISHTI as our validation set:

Dice Metric:

Mean: 0.89671296

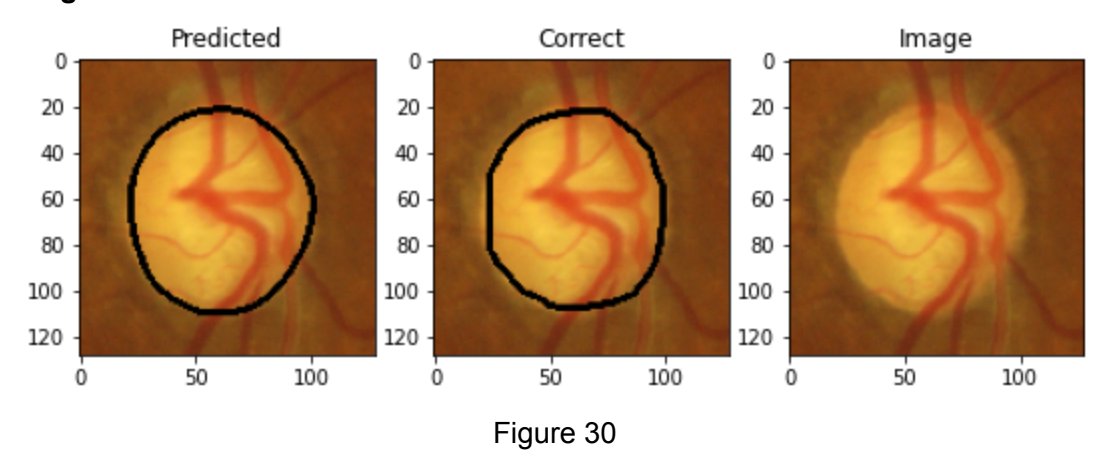
Standard Deviation: 0.056405924

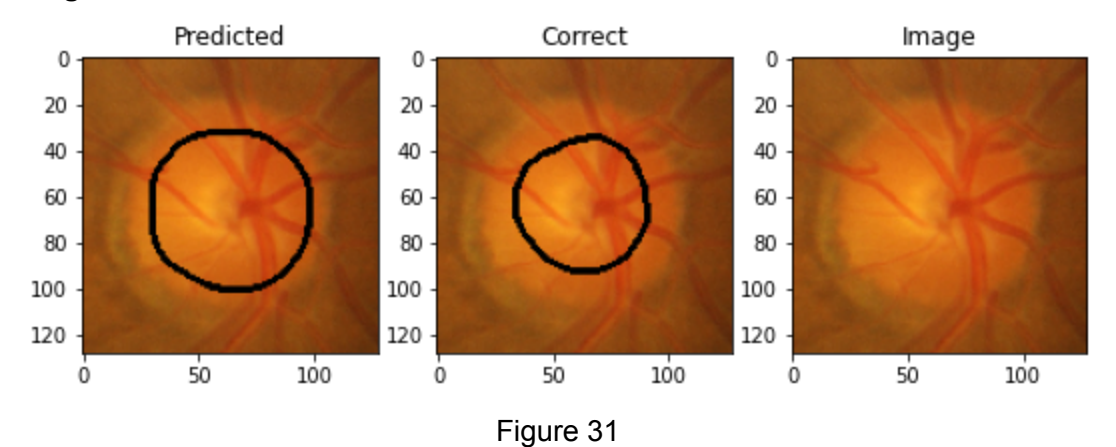
IOU Metric:

Mean: 0.81743157

Standard Deviation: 0.09135907

Model Segmentation with best Dice Score:





Conclusion:

U-Net neural networks can provide results similar or better than existing methods for the tasks of optic disc and cup segmentation on eye fundus images. The same method, applied to both tasks, achieves high quality of segmentation, which proves its applicability to various problems of image recognition. Advantages of the proposed solution also include its simplicity, simple programming with the use of modern frameworks and lowest possible prediction time. Experiments results and visual comparison show that automatic optic disc segmentation can be done at the quality competitive with humans.

However, we can see that the model's disc segmentation metrics are better than it's cup segmentation metrics. We also can see that after epoch 15 the model's cup segmentation accuracy drops significantly and later improves at a very slower rate, Training with high epochs may improve its accuracy. Optic cups are more challenging to recognize, which is supported by the fact that its border is much more subtle. There is a room for improvement for optic cup segmentation, and further research is needed

Consolidated Performance Metric Table:

Metrics after 30 epochs of Training:

Model	Val-Dice-Score	Val-Log-Dice-Loss	Train-Dice-Score	Train-Log-Dice-Loss	
Paper[2]-Unet Disc Segmentation	0.8724	0.1367	0.9406	0.0612	0
Paper[2]-Unet Cup Segmentation	0.6514	0.4303	0.9384	0.0636	1
Paper[3]-Unet Disc Segmentation	0.8905	0.1178	0.9905	0.0095	2
Paper[3]-Unet Cup Segmentation	0.8113	0.2102	0.9909	0.0091	3

Figure 32

Loss and Accuracy Scores on Unseen Test dataset:

N-	Test-Log-Dice-Loss	Test-Dice-Score	Model
0	0.123512	0.883881	Paper[2]-Unet Disc Segmentation
1	0.442063	0.645349	Paper[2]-Unet Cup Segmentation
2	1.052581	0.846409	Paper[3]-Unet Disc Segmentation
3	0.773550	0.778958	Paper[3]-Unet Cup Segmentation

Figure 33

Discussion:

Paper [1] suggests computational ways to segment disc and cup. They mostly rely on histograms and intensity variations. They have developed a formula to retrieve key points from the smoothed histograms which are helpful in thresholding and later segmentation. The drawback of this method is it requires a lot of hyper parameters which are user defined. These hyper parameters must be fine tuned to obtain a state of the art solution. The only parameter they have discovered are the threshold computations, whereas others are left to us. To get an end to end solution we need to know feasible values of all the parameters involved in segmentation. The computational algorithm wrongly classifies few images and these images are affected by the imaging modality. Few images have very high intensity at the edges of the eye which is caused due to imaging modality, as our model solely rely on intensity variations, it identifies the corners as discs which is absurd. These problems suggests us that this way of computational approach cannot be automated and would not perform any good when there is an error with imaging modality.

While looking on the aspects of pure automation we enter into a domain called deep neural networks. Deep neural networks are models which identify it's targets given the right dataset. Neural networks are a black box, because we cannot understand how it creates its own intuition and pattern recognition algorithm. Due to the above mentioned reasons I have chosen approaches that are given in [2] and [3].

The architecture of CNN used for the disc and cup segmentation of the fundus images was derived from the U-Net network. The U-Net exhibits the encoder-decoder architecture where the decoder gradually recovers it. As a result, it produces a pixel-wise probability map instead of classifying an input image as a whole. The U-Net in opposition to other CNN architectures does not require a huge amount of training samples and can be effectively trained with only a few images. This was also in the case of the dataset considered in this study.

[3] model architecture has lot more convolutional layers than [2] model architecture, we know that increased number of convolutional layers mean increased image pattern recognition and learnability of the model, This idea is exactly reflected in Figure 32. We can see that at the end of training, paper [3] u-net architecture has high dice scores than paper [2] u-net architecture in both disc and cup segmentations. We can also identify that Model [3] cup segmentation score is very significantly higher than Model [2]. We earlier mentioned during paper [2] conclusion that there is room for improvement to achieve better scores for cup segmentation and Model [3] here serves its purpose.

We can look at our model's performance on unseen data from Figure 33. We can identify that even though model [3] having higher scores than model [2] in training set, model [3] performs poorer with unseen test set, This may be caused due to the problem of overfitting the training data. However, we can also identify that model [3] again performs significantly higher than model [2] on test set cup segmentation.

We can finally conclude that model [3] performs better with cup segmentation and model [2] performs better with disc segmentation. Model [2] is less complex than [3] as a result it is faster and lighter to use and is very valuable when thinking of end user capability. We can also conclude that CNN models perform better than traditional computational methods and it can also be well automated.

Code:

Dataset:https://drive.google.com/drive/folders/13g62bhqN1JHJ2fky2Xy5avLbZ2Y
LMdwB

Paper[1] - Adaptive

Threshold: https://github.com/thiyagutenysen/Medical-Image-course/blob/master/Adaptive%20T <a href="https://github.com/thiyagutenys/blob/master/bl

Paper[2]-Unet Disc

Segmentation: https://colab.research.google.com/drive/1-nABXPiOSxqW9tg9GLnwvPdKA-o1x37F?usp=sharing

Paper[2]-Unet Cup

Segmentation: https://colab.research.google.com/drive/1aLBbrwxgx9c6vzeJPsu1Ls5E22sFFpdl<a href="https://colab.research.google.com/drive/1aLBbrwxgx9c6vzeJPsu1Ls5E22sFFpdl<a href="https://colab.research.google.com/drive/1aLBbrwxgx9c6vzeJPsu1Ls5E22sFFpdl<a href="https://colab.research.google.com/drive/1aLBbrwxgx9c6vzeJPsu1Ls5E22sFFpdl<a

Paper[3]-Unet Disc

Segmentation: https://colab.research.google.com/drive/1gYlyLKgvKR9inxTizAuBITIx9WP1wEQx ?usp=sharing

Paper[3]-Unet Cup

Segmentation: https://colab.research.google.com/drive/11ZsJKN2fNQ2AictxEZneBoDt_fJyR_ZO http

References:

- [1] An adaptive threshold based algorithm for optic disc and cup segmentation in fundus images
- [2] Optic Disc and Cup Segmentation Methods for Glaucoma Detection with Modification of U-Net Convolutional Neural Network
- [3] <u>U-Net: Convolutional Networks for Biomedical Image Segmentation</u>